Journal of Computer Science and Artificial Intelligence
ISSN: 3078-8242 (Print), ISSN: 3078-2309 (Online) | Vol. 8, No. 3, 2026

Condition Assessment of Circuit Breaker Mechanical Performance During Opening and Closing Operations Using Adaptive Machine Learning

Junyuan Cao *

Faculty of Electrical engineering, Shanghai University of Electric Power, Shanghai, 200090, China

* **Corresponding author**: (Email: iutr7837@gmail.com)

Abstract: The mechanical performance of circuit breakers during opening and closing operations directly affects the safety and stability of power systems. However, conventional threshold-based methods cannot adequately represent nonlinear relationships among multiple mechanical parameters and have limited adaptability to equipment differences and changing operating conditions. This study proposes an adaptive machine learning method for circuit breaker mechanical condition assessment. Opening and closing times, operating velocities, contact travel, overtravel, three-phase asynchronism, and the cumulative number of operations are processed through data cleaning, normalization, and deviation calculation to construct a mechanical performance feature set. Circuit breaker conditions are classified into normal, attention, abnormal, and severe levels. An adaptive XGBoost model combining data-driven and model-driven feature weights is then developed. Bayesian optimization determines key model parameters, while a recent-sample-weighted updating mechanism improves adaptability to data-distribution changes. The model generates a condition level and comprehensive health score, and SHAP analysis explains individual feature contributions. The proposed model achieves an Accuracy of 0.950, an F1-score of 0.944, and an AUC of 0.983, outperforming support vector machine, random forest, and conventional XGBoost. Under a 40% distribution shift, adaptive updating increases the F1-score from 0.796 to 0.891. Opening time, closing velocity, contact overtravel, and opening velocity are identified as the most influential indicators. The method can identify gradual deterioration and provide interpretable evidence for condition-based maintenance.

Keywords: Circuit breaker, Mechanical performance, Condition assessment, Adaptive machine learning.

1. Introduction

Circuit breakers are essential control and protection devices in power systems, performing routine load switching, fault-current interruption, and electrical isolation. Their operational reliability is therefore directly associated with the safety and stability of power grids. Opening and closing operations require coordinated motion of the operating mechanism, energy-storage unit, transmission components, and contact system. As the number of operations increases, repeated mechanical impacts, component wear, lubrication degradation, and environmental exposure may gradually lead to spring fatigue, mechanism jamming, enlarged transmission clearances, contact wear, and three-phase operating asynchronism. These conditions may manifest as prolonged operating times, reduced contact velocities, travel deviations, or failure to open or close. Conventional periodic maintenance and threshold-based assessment methods compare individual mechanical parameters with predefined limits. Although straightforward, they cannot adequately describe nonlinear interactions among multiple indicators or reliably identify incipient degradation before an alarm threshold is reached. Accurate and timely assessment using operational and mechanical test data is therefore fundamental to condition-based maintenance and prevention of unexpected failures.

In recent years, vibration signals, opening and closing coil currents, contact travel curves, and operating-time measurements have increasingly been used for circuit breaker condition monitoring. Time-domain, frequency-domain, wavelet, and modal decomposition techniques can extract features associated with mechanical events, while support vector machines, random forests, ensemble learners, and deep neural networks have been applied to fault identification [1–4]. Machine learning captures complex relationships between multidimensional monitoring features and equipment condition, but most existing studies focus on predefined faults under controlled laboratory conditions and use fixed feature sets and parameters [5–7]. Variations in circuit breaker type, control voltage, environment, and operating stage may introduce distribution shifts and reduce offline model performance. Field fault samples are also scarce and imbalanced, making complex deep models susceptible to overfitting [8–10]. Developing an assessment model that adjusts its features and parameters in response to changing data while producing interpretable condition levels and health scores remains an important challenge.

To address these limitations, this study proposes an adaptive machine learning method for assessing circuit breaker mechanical performance during opening and closing operations. Key mechanical indicators are normalized and converted into deviation features to establish four condition levels. An optimized XGBoost model combines adaptive feature weighting, Bayesian parameter selection, and recent-sample-weighted updating. It simultaneously outputs a mechanical condition level and comprehensive health score, while SHAP analysis identifies the principal contributors to deterioration. Comparisons with support vector machine, random forest, and conventional XGBoost, together with distribution-shift and ablation experiments, are used to evaluate accuracy, stability, adaptability, and interpretability.

2. Materials and Methods

2.1. Mechanical Performance Data and State Classification

Circuit breaker opening and closing operations are initiated by energy release from the operating mechanism and completed by contact movement through the transmission mechanism. Wear, fatigue, looseness, and jamming alter this energy-transfer process and are reflected in operating time, contact velocity, travel, and three-phase synchronization. Opening time, closing time, opening velocity, closing velocity, contact travel, overtravel, opening asynchronism, and closing asynchronism were selected as principal features. Control voltage and the cumulative number of operations were included as auxiliary variables describing operating conditions and accumulated degradation. As shown in table 1.

Table 1. Mechanical performance indicators of circuit breakers

Category	Indicator	Symbol	Mechanical condition represented
Operating time	Opening time	T_o	Release response and opening mechanism
Operating time	Closing time	T_c	Closing coil and mechanism output
Velocity	Opening velocity	V_o	Opening spring energy and resistance
Velocity	Closing velocity	V_c	Closing spring and transmission
Displacement	Contact travel	L_t	Transmission integrity and contact movement
Displacement	Contact overtravel	L_e	Contact wear and contact pressure
Synchronization	Opening asynchronism	ΔT_o	Three-phase opening consistency
Synchronization	Closing asynchronism	ΔT_c	Three-phase closing consistency
Operating condition	Control voltage	U_c	Operating mechanism input
Operating condition	Operation count	N	Accumulated mechanical degradation

Raw records were checked for completeness. A small number of missing observations were replaced by the median of the corresponding training feature, whereas isolated sensor or transmission anomalies were identified using the interquartile-range criterion. Because different circuit breaker types may have different nominal values, each parameter was expressed relative to its normal reference and permissible limit:

$$d_{ij} = \min\left(1, \frac{|x_{ij} - x_{j,0}|}{|x_{j,\lim} - x_{j,0}| + \varepsilon}\right) \quad (1)$$

Where x_{ij} is feature j of sample i, $x_{j,o}$ is its factory reference or normal operating value, x_j, lim is its permissible limit, and ε is a small constant. A larger d_{ij} indicates a greater departure from normal performance. Z-score normalization was then applied using statistics obtained exclusively from the training set:

$$z_{ij} = \frac{x_{ij} - \mu_j}{\sigma_j} \quad (2)$$

The initial comprehensive deviation was calculated from the weighted feature deviations:

$$D_i = \sum_{j=1}^{m} w_j \, d_{ij}, \qquad \sum_{j=1}^{m} w_j = 1 \quad (3)$$

Table 2. Mechanical performance condition levels

Condition level	Deviation interval	Description	Recommended action
Level I	0 ≤ D < 0.25	Normal and stable performance	Routine monitoring
Level II	0.25 ≤ D < 0.50	Slight parameter deviations	Shorten inspection interval
Level III	0.50 ≤ D < 0.75	Evident deterioration	Targeted inspection
Level IV	0.75 ≤ D ≤ 1.00	High risk of operating failure	Maintenance or removal from service

As shown in table 2. Samples near adjacent boundaries were reviewed using historical trends and maintenance records to reduce deterministic labeling errors. The dataset was divided into training, validation, and test subsets at 70%, 15%, and 15%, respectively, using stratified sampling to retain the four-level distribution.

2.2. Adaptive Machine Learning-Based Assessment Model

XGBoost was used as the base learner because its gradient-boosted trees can represent nonlinear relationships and feature interactions in medium-sized structured datasets. The model sequentially fits residual errors, with the regularized objective function expressed as:

$$\mathcal{L}^{(t)} = \sum_{i=1}^{n} l\left(y_i, \hat{y}_i^{(t-1)} + f_t(x_i)\right) + \Omega(f_t) \quad (4)$$

Where l(·) is the multiclass loss, f_t is the t-th decision tree, and $\Omega(f_t)$ controls tree complexity. Adaptive mechanisms were introduced at feature and model levels. A data-driven weight was first calculated from mutual information between each feature and condition label:

$$w_j^d = \frac{MI(X_j, Y)}{\sum_{k=1}^{m} MI(X_k, Y)} \quad (5)$$

A model-driven weight was obtained from the cumulative splitting gain G_j generated by XGBoost:

$$w_j^m = \frac{G_j}{\sum_{k=1}^{m} G_k} \quad (6)$$

The final feature weight combined these two components:

$$w_j = \alpha w_j^d + (1 - \alpha) w_j^m \quad (7)$$

Where α was determined on the validation set. The learning rate, tree depth, number of estimators, subsampling ratio, column-sampling ratio, and regularization coefficients were selected through Bayesian optimization with stratified five-fold cross-validation:

$$\theta^* = \underset{\theta}{\operatorname{argmax}} F_{1,\mathrm{macro}}(\theta) \quad (8)$$

To accommodate temporal data drift, the model was updated when the estimated feature-distribution shift or continuous assessment error exceeded a predefined threshold. Historical and recent samples were assigned exponentially decaying temporal weights:

$$\lambda_i = \exp\left[-\beta(t_{\mathrm{now}} - t_i)\right] \quad (9)$$

Where t_i is acquisition time, tnow is update time, and β is the decay coefficient. Recent observations therefore have greater influence while historical information prevents unstable updates. The model outputs probabilities p_{ik} for four condition levels. Baseline scores of 100, 75, 45, and 15 were assigned to Levels I–IV, and the comprehensive health score was calculated as:

$$S_i = \sum_{k=1}^{4} p_{ik}\, q_k \quad (10)$$

The final assessment contains the predicted condition level, health score, prediction confidence, and dominant contributing features.

2.3. Model Evaluation

Support vector machine, random forest, and conventional XGBoost were used as baselines under identical data partitions and preprocessing procedures. Conventional XGBoost used fixed features and no recent-sample updating. Accuracy, macro-averaged Precision, Recall, F1-score, and multiclass AUC were used for evaluation. Their definitions are given in Equations (11)–(14), where K = 4 and TP_k, FP_k, and FN_k denote true positives, false positives, and false negatives for level k. As shown in table 3.

$$\text{Accuracy} = \frac{\sum_{k=1}^{K} TP_k}{N} \quad (11)$$

$$\text{Precision}_{\mathrm{macro}} = \frac{1}{K}\sum_{k=1}^{K}\frac{TP_k}{TP_k+FP_k} \quad (12)$$

$$\text{Recall}_{\mathrm{macro}} = \frac{1}{K}\sum_{k=1}^{K}\frac{TP_k}{TP_k+FN_k} \quad (13)$$

$$F_{1,\mathrm{macro}} = \frac{1}{K}\sum_{k=1}^{K}\frac{2P_kR_k}{P_k+R_k} \quad (14)$$

Table 3. Baseline models and principal characteristics

Model	Principal characteristic	Adaptive weighting	Optimization	Updating
SVM	Kernel-based boundary	No	Yes	No
Random Forest	Randomized tree ensemble	No	Yes	No
XGBoost	Gradient-boosted trees	No	Yes	No
Proposed model	Adaptive weighted XGBoost	Yes	Yes	Yes

Ablation experiments separately removed adaptive feature weighting, Bayesian optimization, and sample updating. SHAP values quantified the direction and magnitude of each feature's contribution to the model output.

3. Results and Discussion

3.1. Model Performance Comparison

All models used identical inputs and data partitions. Each experiment was repeated ten times, and average results are reported in Table 4. The proposed model achieved the best performance for every metric, with an Accuracy of 0.950, F1-score of 0.944, and AUC of 0.983. Relative to conventional XGBoost, the F1-score and AUC increased by 3.4 and 1.8 percentage points, respectively. This improvement indicates that adaptive weighting reinforces state-sensitive information and Bayesian optimization balances fitting capability with generalization. As shown in figure 1.

Table 4. Mechanical condition assessment performance of different models

Model	Accuracy	Precision	Recall	F1-score	AUC
SVM	0.862	0.848	0.836	0.842	0.918
Random Forest	0.895	0.887	0.878	0.882	0.946
XGBoost	0.921	0.914	0.906	0.910	0.965
Proposed model	0.950	0.946	0.942	0.944	0.983

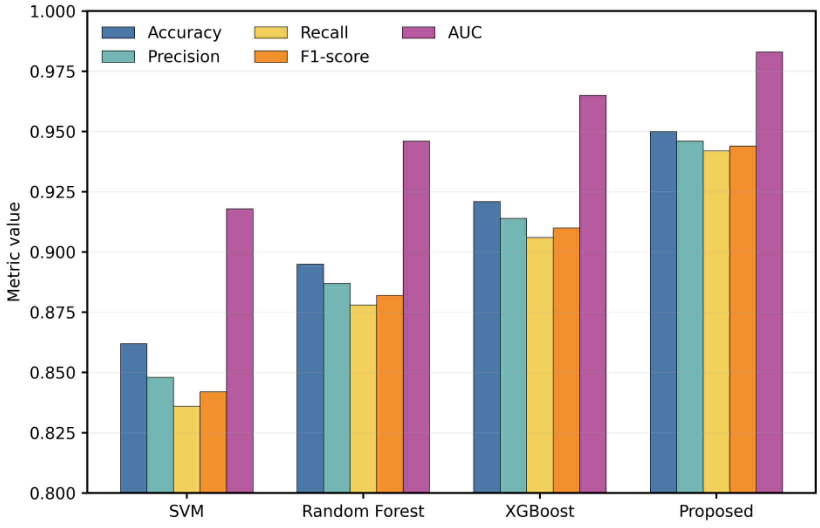

Figure 1. Performance comparison of the condition assessment models

Figure 2 presents the confusion matrix for 240 test samples, of which 228 were correctly classified. Most errors occurred between adjacent levels because samples close to a condition boundary can have similar parameter distributions. No direct confusion occurred between Levels I and IV, indicating clear separation between stable performance and severe deterioration.

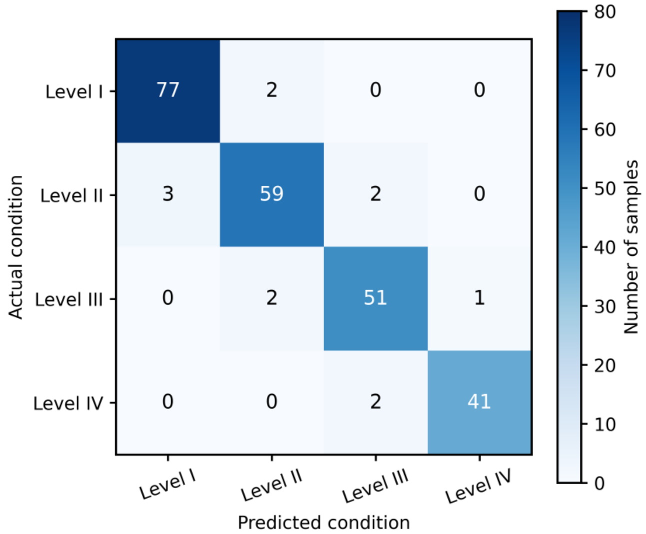

Figure 2. Confusion matrix of the proposed condition assessment model

3.2. Mechanical Condition Assessment Results

Mechanical data from 60 consecutive operation batches were evaluated to examine gradual deterioration. The initial health score remained above 90 and was classified as Level I. As operation count increased, the score gradually entered Levels II and III. Short-term fluctuations were superimposed on the long-term decline because control voltage, environment, and lubrication can cause temporary variations, whereas spring fatigue, contact wear, and increased transmission clearance produce persistent deterioration. As shown in figure 3.

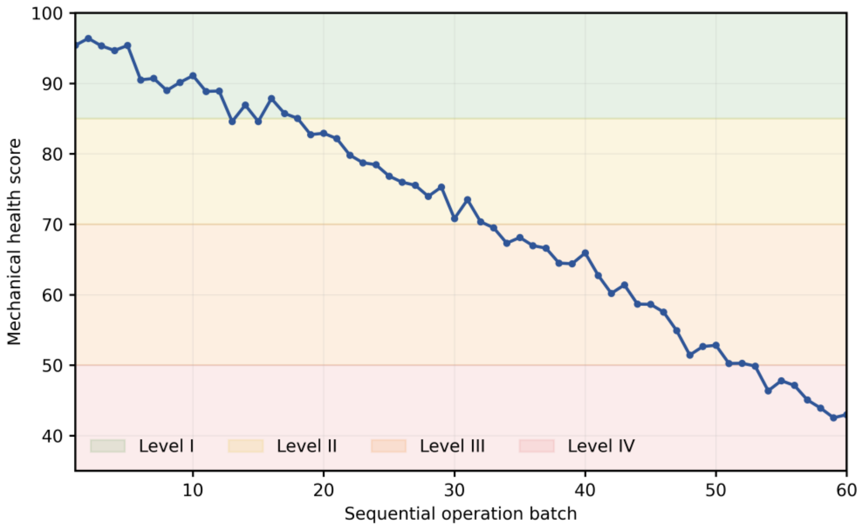

Figure 3. Evolution of the mechanical health score over sequential operation batches

The comprehensive score captures accumulated deviations before every individual parameter exceeds its limit. Table 5 illustrates representative cases. Combining a score, level, confidence, and dominant feature provides more actionable information than a condition label alone and can direct inspection toward the release mechanism, spring, transmission components, or contact system.

Table 5. Mechanical performance assessment of representative samples

Sample	Main parameter variation	Score	Level	Confidence	Action
A	Parameters close to references	94.6	I	0.972	Routine monitoring
B	Reduced closing velocity; overtravel deviation	78.3	II	0.914	Shorten interval
C	Prolonged opening; increased asynchronism	61.5	III	0.938	Targeted inspection
D	Multiple parameters near/beyond limits	31.7	IV	0.981	Immediate maintenance

3.3. Adaptability and Feature Contribution Analysis

Distribution shifts were introduced to simulate variations in control voltage, ambient conditions, equipment type, parameter baselines, and operating stage. Without updating, the F1-score decreased from 0.944 to 0.796 as shift intensity reached 40%. After recent-sample weighting and model updating, the F1-score remained 0.891, an improvement of 9.5 percentage points. The benefit increased with shift intensity, confirming that updating is most valuable when operating conditions and data characteristics change. As shown in table 6 and figure 4.

Table 6. F1-scores before and after adaptive updating.

Distribution shift	Before updating	After updating	Improvement
0%	0.944	0.944	0.000
10%	0.918	0.936	0.018
20%	0.886	0.925	0.039
30%	0.842	0.909	0.067
40%	0.796	0.891	0.095

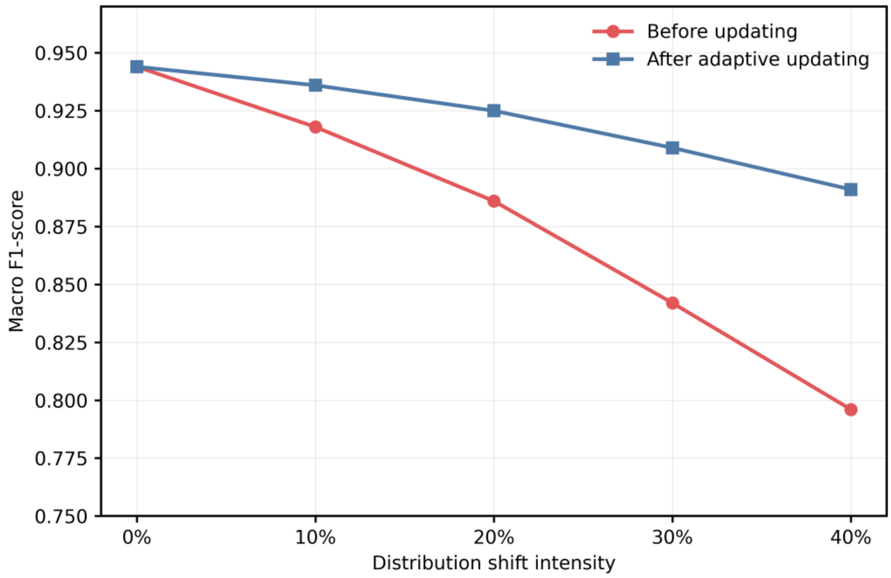

Figure 4. F1-score before and after adaptive updating under distribution shifts

Removing any adaptive component reduced performance (Table 7). The largest decrease occurred when sample updating was removed, demonstrating the importance of recent observations under changing conditions. The complete model exceeded conventional XGBoost, showing that improvement resulted from the combined contributions of feature adaptation, parameter optimization, and updating rather than a single tuning step.

The SHAP results in Figure 5 identify opening time as the most influential feature, followed by closing velocity, overtravel, and opening velocity. These indicators describe release response, closing-mechanism output, contact wear, and spring energy. Operation count also contributed substantially, reflecting cumulative mechanical degradation. Control voltage had lower global importance but remained useful for distinguishing temporary input-condition effects from persistent mechanical abnormalities.

Table 7. Ablation results of the proposed model.

Model configuration	Accuracy	F1-score	AUC
Complete model	0.950	0.944	0.983
Without adaptive feature weighting	0.936	0.929	0.974
Without Bayesian optimization	0.939	0.933	0.976
Without sample updating	0.931	0.924	0.970
Conventional XGBoost	0.921	0.910	0.965

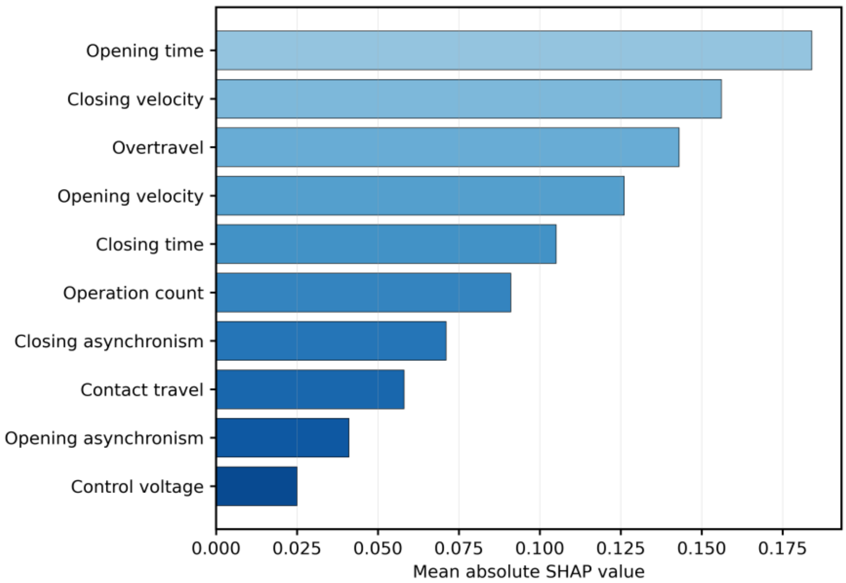

Figure 5. Mean absolute SHAP values of the mechanical performance indicators

4. Conclusion

This study proposed an adaptive machine learning method for assessing circuit breaker mechanical performance during opening and closing operations. A four-level assessment system was established using operating times, velocities, travel, overtravel, phase asynchronism, and operation count. Data-driven and model-driven feature weights were combined, while Bayesian optimization and recent-sample updating improved adaptability to equipment differences and changing distributions. The model produced a condition level, health score, and interpretable feature contributions.

The proposed model achieved an Accuracy of 0.950, an F1-score of 0.944, and an AUC of 0.983, outperforming SVM, random forest, and conventional XGBoost. Under a 40% distribution shift, updating increased the F1-score from 0.796 to 0.891. Opening time, closing velocity, overtravel, and opening velocity were the most influential indicators. Future work will incorporate long-term field data from multiple voltage levels and operating mechanisms and fuse vibration, acoustic, and coil-current signals. Transfer learning, online incremental learning, and digital twins may further support cross-device assessment and remaining-life prediction.

References

[1] Zhang, J., Wu, Y., Xu, Z., et al. (2022). Fault diagnosis of high voltage circuit breaker based on multi-sensor information fusion with training weights. Measurement, 192, 110894.

[2] Wang, Y., Yan, J., Ye, X., et al. (2022). Few-shot transfer learning with attention mechanism for high-voltage circuit breaker fault diagnosis. IEEE Transactions on Industry Applications, 58(3), 3353–3360.

[3] Ye, X., Yan, J., Wang, Y., et al. (2022). A novel U-Net and capsule network for few-shot high-voltage circuit breaker mechanical fault diagnosis. Measurement, 199, 111527.

[4] Ye, X., Yan, J., Wang, Y., et al. (2022). A novel capsule convolutional neural network with attention mechanism for high-voltage circuit breaker fault diagnosis. Electric Power Systems Research, 209, 108003.

[5] Yan, J., Wang, Y., Yang, Z., et al. (2023). Few-shot mechanical fault diagnosis for a high-voltage circuit breaker via a Transformer–convolutional neural network and metric meta-learning. IEEE Transactions on Instrumentation and Measurement, 72, 1–11.

[6] Wu, Y., Zhang, J., Yuan, Z., et al. (2023). Fault diagnosis of medium voltage circuit breakers based on vibration signal envelope analysis. Sensors, 23(19), 8331.

[7] Liu, Q., Wang, Y., Liu, X., et al. (2024). Mechanical defect diagnosis of high voltage circuit breakers based on the combination of stroke curve and current signal. Electrical Engineering, 106(1), 1093–1103.

[8] Li, T., Xia, Y., Pang, X., et al. (2024). Mechanical fault diagnosis of high voltage circuit breaker using multimodal data fusion. PeerJ Computer Science, 10, e2248. https://doi.org/10.7717/peerj-cs.2248

[9] Yang, Q., & Liao, Y. (2024). A novel mechanical fault diagnosis for high-voltage circuit breakers with zero-shot learning. Expert Systems with Applications, 245, 123133.

[10] Liu, Y., Li, H., Wang, H., et al. (2025). A fault diagnosis of high voltage circuit breakers with small samples using a PCA-cascade forest algorithm. Energy Reports, 13, 6190–6200.